Optical Fiber Technology 85 (2024) 103794

Contents lists available at ScienceDirect

Optical Fiber Technology

journal homepage: www.elsevier.com/locate/yofte

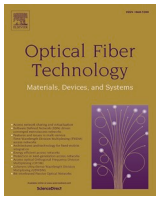

Regular Articles

Carbon-coated fiber for optoelectronic strain and vibration sensing

Josu Amorebieta [a,*], Joao Pereira [b], Carolina Franciscangelis [b], Gaizka Durana [c], Joseba Zubia [c], Joel Villatoro [c,d], Walter Margulis [b]

[a] Department of Applied Mathematics, University of the Basque Country UPV/EHU, Ingeniero Torres Quevedo Plaza, 1, 48013 Bilbao, Spain
[b] RISE Fiber Optics, RISE Research Institutes of Sweden, Electrum 236, Kista, Stockholm, SE 164 40, Sweden
[c] Department of Communications Engineering, University of the Basque Country UPV/EHU, Ingeniero Torres Quevedo Plaza, 1, 48013, Bilbao, Spain
[d] Ikerbasque, Basque Foundation for Science, Bilbao 48013, Spain

ARTICLE INFO

Keywords:
Optical fiber
Optical sensor
Carbon coating
Low coherence interferometer
Strain
Vibration
Impedance

ABSTRACT

In this article, we report on a carbon-coated optical fiber that is suitable to be used simultaneously as a transmission medium and as a sensor. It consists of a standard single mode fiber (SMF) sleeved in two layers of coating, which provide protection and isolation from external elements. The inner layer is made of carbon, whereas the outer is made of polymer. When the fiber is subjected to mechanical stress, the electrical resistance of the carbon layer changes accordingly. The voltage variations caused by the former can be measured with high accuracy and without interfering with the light propagating through the SMF. In this work, the feasibility of this operating principle is demonstrated in a low coherence Michelson interferometer in which electrical and optical signals were measured simultaneously and compared to each other. Results indicate that electrical measurements are as precise as the optical ones and with linear behavior, reaching a sensitivity of 1.582 mV/με and able to detect vibrations down to 100 mHz.

1. Introduction

Optical fibers play a significant role in telecommunications [1,2] and sensing applications [3,4]. On the one hand, for telecommunications, they provide high bandwidth and low attenuation rates over long distances, which results in links with low latency rates and high capacity, stability and speed [5,6]. On the other hand, for sensing, optical fibers provide high sensitivity, electromagnetic immunity, lightweight and small size. Thanks to these characteristics, they can be deployed in harsh environments such as nuclear plants, embedded in aircraft composites for internal inspections, or integrated with ease in infrastructures as gas pipes or high-voltage lines without affecting their performance [7–10].

Commonly, for the aforementioned applications, polymer-coated glass optical fibers are installed. Polymeric coatings provide high short-term strength, but in humid environments, long-term strength degradation occurs and, thus, hermetically coated optical fibers become of interest. To that end, additional materials are incorporated to optical fibers in order to expand their functionalities and applications [11], and to improve their features so that they can exhibit high resistance to moisture attack, or they can withstand high temperatures [12]. Carbon represents one of those materials that act as a hermetic seal to prevent the presence of hydrogen in the core [13], but its use would also be of great interest for other applications in the field of sensing. Ultimately, having an optical fiber capable of managing both tasks –within telecommunications and sensing- simultaneously results of great interest, as it would allow optimizing resources, minimizing the level of intrusiveness and reducing the installation complexity.

In this work, we report on a carbon-coated optical fiber that takes advantage of its conductive coating to act as an electronic sensor as well. It consists of a standard single mode fiber (SMF) sleeved in a coating that is comprised of two layers. The inner and outer layers are made of carbon and polymer, respectively, in order to provide isolation and protection against external elements. When such a fiber is subjected to mechanical stress or bending, the light guided through the SMF core remains unaltered whereas the physical properties of the carbon of the inner layer of the coating change, thereby modifying its electrical resistance. The latter is proportional to the strain applied to the fiber. Thus, one can use the minimally invasive character of the fiber to sense the strain through the electrical resistance of the carbon coating, without affecting the intensity of the guided light.

The feasibility of this operating principle is demonstrated through the measurement of strain and vibrations in a low coherence Michelson

* Corresponding author.
E-mail address: josu.amorebieta@ehu.eus (J. Amorebieta).

https://doi.org/10.1016/j.yofte.2024.103794
Received 6 February 2024; Received in revised form 21 March 2024; Accepted 8 April 2024
Available online 10 April 2024

interferometer in which the reference arm consisted of standard SMF and the arm exposed to the mechanical stress consisted of carbon-coated fiber. Our setup allowed comparing electrical measurements obtained from the carbon coating with optical measurements from the interferometer, which are well known for their accuracy and reliability. Results indicate that electrical measurements behaved linearly in all the tested range, and that they are as accurate as optical measurements, reaching a sensitivity of 1.582 mV/με in the strain range from 0 to 1552.8 με, and able to detect vibrations down to 100 mHz.

2. Materials and methodology

The schematic of the experimental setup used in this work is shown in Fig. 1.

In the following subsections the carbon-coated fiber and the methodology for electrical and optical measurements are described.

2.1. The fiber

The carbon-coated fiber used in this work has been designed and fabricated at RISE Research Institutes of Sweden. It has a diameter of 250 μm and it is composed of an SMF commonly used in telecommunications (numerical aperture of 0.14 at 1550 nm) sleeved in two different coatings of identical thickness (31.25 μm each) (see Fig. 2). The inner coating is made of carbon, whereas the outer coating is made of polymer. Thanks to the former, this fiber can be deployed in harsh environments such as the ones with high levels of radiation, corrosive materials or undersea [14,15], as it avoids the attenuation caused by hydrogen in the absorption band close to the transmission window around 1550 nm [16]. The polymer coating provides protection against environmental factors and electrically isolates the conductive layer.

The use of a carbon coating as a tool to enhance the sensing performance of SMFs has been reported already [17,18]. However, in this work the electrical resistance of the carbon coating itself has been used for sensing purposes, as its variations can be converted into a voltage level and measured with high accuracy, linking it directly to the parameter causing the mechanical stress to the fiber [19]. Although the electrical resistance of the carbon layer depends on the fabrication process [20], and the mechanical properties of the carbon-coated optical fiber depend on the coating structure and roughness [21], in the present research they all remain constant. Thus, in addition to providing protection, the carbon coating could be also used for sensing, whereas the SMF could be used simultaneously for the transmission of light, as optical and electrical signals do not interfere with each other.

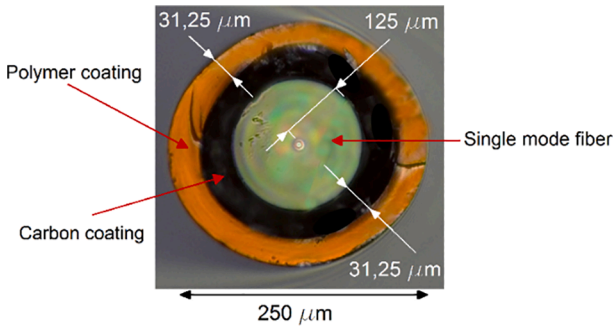

Fig. 2. Cross-section of the manufactured carbon-coated fiber.

2.2. Electrical measurements

Regarding electrical measurements, they were carried out on a Wheatstone bridge, as the latter is a very mature, reliable and sensitive technique for voltage variation measurements. It was responsible for converting the strain-dependent resistance into voltage and it was connected to an oscilloscope (Tektronix TDS 3034) to display and record the incoming signal (see Fig. 1). To that end, the carbon-coated fiber was located at one of the legs of the bridge circuit, which was configured to be balanced when the fiber was resting at 0 με, which was taken as reference point. In that case, the voltage drop in the two edges of the bridge is identical:

$$V_{R2} - V_{R3} = 0 \tag{1}$$

where R_2 is a standard resistance (R_1 is identical to R_2, and both resistances conform one of the legs of the bridge), and R_3 is a variable resistance so that the bridge can be easily and precisely adjusted to be balanced for different carbon-coated fiber samples (see Fig. 1), whose resistance is named *RCarbonFiber*.

Such configuration allows measuring very small resistance variations. When the fiber is subjected to any effect that causes a change in its impedance, the Wheatstone bridge is unbalanced, and the voltage dif-

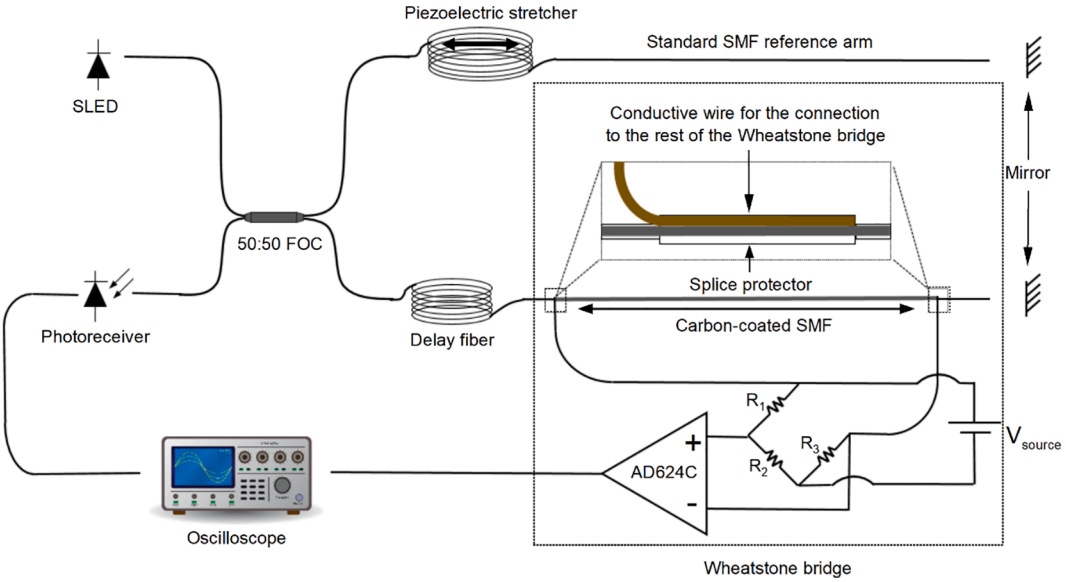

Fig. 1. Schematic of the experimental setup. The mirror stands at a certain distance from both arms, where the light exiting both fibers is reflected and couples again in both fibers. R stands for Resistance and Vsource is the voltage supply, fixed at 24 V.

ference can be measured and calculated as:

$$V_{output} = V_{R2} - V_{R3} = V_{source}\left(\frac{R_2}{R_2 + R_1} - \frac{R_3}{R_3 + R_{CarbonFiber}}\right) \quad (2)$$

where V_{source} is fixed to 24 V. Moreover, with this configuration, it could be guaranteed that the order of magnitude of the current through the carbon-coated fiber would be of mA, avoiding any damage to the carbon or the polymer coatings of the fiber.

Afterwards, in order to amplify the slight voltage variations, an instrumental amplifier (AD624C) was connected at its output and configured to provide a gain of 500 (see Fig. 3).

Thus, the voltage displayed in the oscilloscope can be expressed as:

$$V_{oscilloscope} = 500 V_{output} \quad (3)$$

Regarding the electrical connection between the electric components of the bridge and the carbon-coated fiber, it was made at both ends of the latter. For that purpose, the polymer coating was removed at those endpoints. As a result of it, part of the carbon coating was also removed, reducing its thickness to approximately 3 μm along a fiber length of 5 cm (see Fig. 4).

Thereafter, a fine copper wire was wound around a ~ 2 cm-long section of the carbon-coating without polymer in order to improve the electrical contact. Lastly, a conventional splice protector was thermally collapsed on the arrangement. This ensured low electrical resistance and rugged mechanical support for the fiber attachment to the experimental setup. The carbon coated fiber and SMF were fusion spliced at both ends using a standard fusion splicer. The thin layer of carbon had not impact during the splicing process.

2.3. Low coherence interferometer

Optical measurements were carried out in a low coherence Michelson fiber interferometer, as this experimental configuration allows measuring optical and electrical signals simultaneously for comparison purposes in order to evaluate the accuracy and reliability of electrical measurements. Low coherence interferometry is a mature non-contact sensing technology, similar to 1D-optical coherence tomography, that provides high sensitivity, resolution and reliability [22–24]. In fact, it has been frequently used in the industry for the detection and/or measurement of parameters of interest such as pressure, temperature, etc. [25–28], and also in medical and biological applications [29–31].

Briefly, when a low-coherence light source is used in such reflectometers, the interference fringe contrast peaks when the arm lengths are exactly equal, and becomes rapidly small as the probe arm becomes longer or shorter than the reference arm. Thus, the interference pattern can be displayed by periodically stretching and releasing the reference arm in a controlled way. In this pattern, periodical constructive and destructive interferences are shown when maximum and minimum intensities are displayed, respectively. As any disturbance applied to the probe arm (such as temperature or strain, for instance) shifts the position of the maximum of the fringe pattern, the interferometer is able to read in real time and with micron-precision small shifts caused by the aforementioned disturbances.

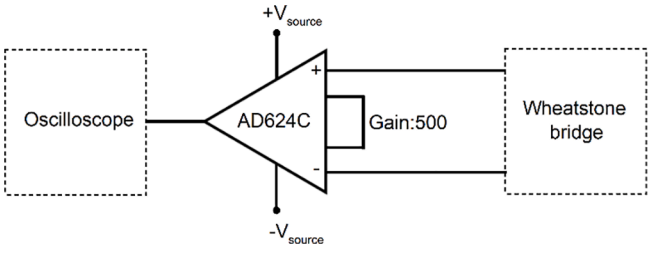

Fig. 3. Configuration of the AD624C for a gain of 500.

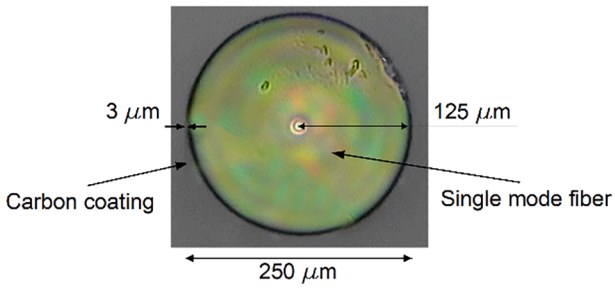

Fig. 4. Cross-section of the carbon-coated fiber once the polymer coating is removed.

In this work, a commercial piezo stretcher was driven at 50 Hz, which elongated the reference arm of the interferometer by up to 1 mm repetitively and allowed showing the pattern in which periodical constructive and destructive interferences are shown. The low coherence interferometer used a super luminescent diode (SLED, DenseLight Semiconductors) whose light was split into two independent paths with nearly identical length by means of a 50:50 fiber optic coupler (FOC). As it can be seen in Fig. 1, in this experimental setup, only the probe path included the carbon-coated fiber. A mirror located at approximately the same distance from the GRIN-lensed fiber ends of both paths reflected the light back into the interferometer arms. Lastly, a photoreceiver (New Focus 2053) captured the interference of both reflected beams, which was displayed and recorded in the same oscilloscope (Tektronix TDS 3034) used for electrical measurements.

3. Results and discussion

3.1. Strain measurements

The first test consisted in applying several strain cycles from 0 to 1552.8 με to the carbon-coated fiber. For that purpose, the fiber was fixed horizontally, with one of its ends attached to a micrometric displacement platform that allowed stretching and compressing it manually in controlled steps, and the other end attached to a fixed platform so that the fiber was steady at this point. The length of the carbon-coated fiber section in the air and its electrical resistance at the reference level of 0 με were 96.6 cm and 430.95 kΩ, respectively (see Fig. 5).

Regarding optical measurements, the range of the interferometer covered a strain span of 207.05 με, as this was the maximum displacement of the spectrum that could be displayed in the oscilloscope without overlapping with adjacent patterns. The latter are caused by the low coherence and broadband light source used in the setup, which only produces interference fringes when the difference between the two paths of interfering light is less than the width of its coherence function. This means that as the path length difference (or delay in time) changes, several identical fringes will appear at the interferometer output. The difference between the adjacent maximums is a very precise indicator of the moment when the interferometer paths are equal for any given reflection [32]. Moreover, the broadband light source that was used in the experiments was a superluminiscent diode whose spectrum is not Gaussian, and the less Gaussian the source spectrum is, the more frequently peaks appear in the time domain [33]. As a result, the range for optical measurements was significantly shorter than the electrically measurable span, which was of 1552.8 με. Thus, in order to compare optical and electrical signals, the interferometer was configured in such a way that its range started at 1345.75 με and ended at 1552.8 με. In this region, 5 equidistant strain points were measured (every 51.76 με). On the other hand, in the electrical measurements and in the range from 0 to 1035.2 με, 3 strain points every 517.6 με were considered.

The strain cycles carried out for this test and their results for electrical and optical measurements are summarized in Fig. 6. For electrical

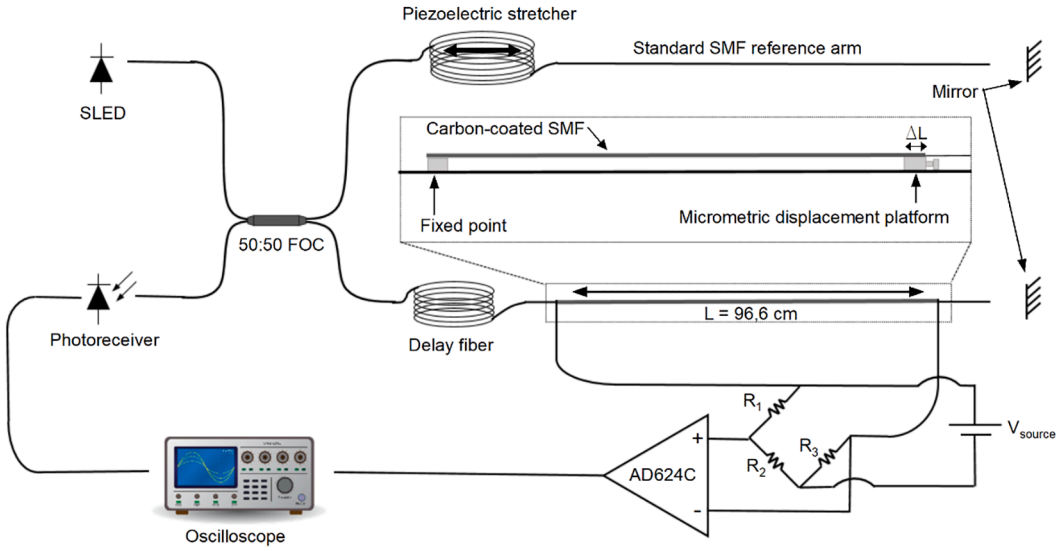

Fig. 5. Schematic of the experimental setup for strain measurements.

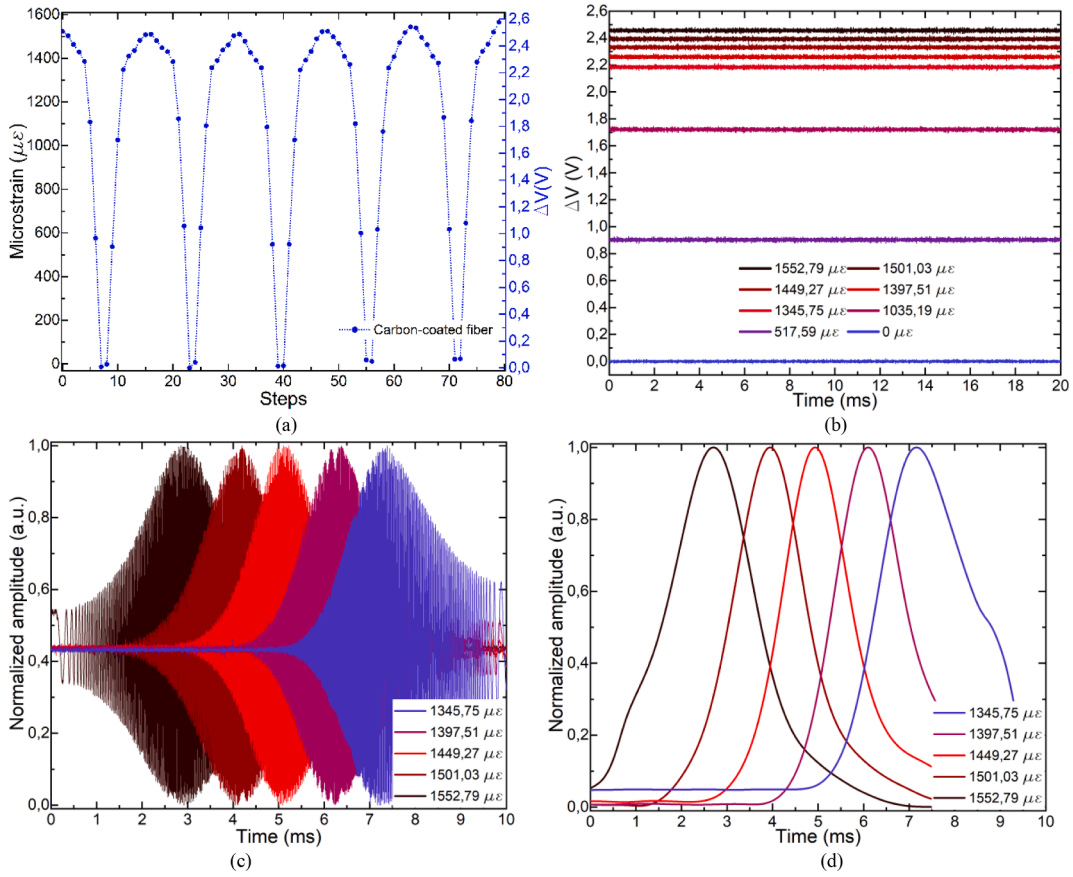

Fig. 6. (a) Electrically measured strain cycles (b) Average of the voltage variation at each tested point (c) Optically measured strain cycles (d) Average of the optical measurements at each tested point.

measurements, in Fig. 6a, 5 consecutive strain cycles are shown, whereas in Fig. 6b the average of the voltage variation at each tested point is shown. Such variation was calculated as the difference between the average of the recorded voltage at each tested point and the average of the reference voltage ($<\Delta V>=<V>-<V_{ref}>$). For optical measurements, the envelope of the upper half of the fringe pattern shown in Fig. 6c was acquired from the oscilloscope and a locally estimated scatterplot smoothing (loess) filter was applied to it (see Fig. 6d).

For both electrical and optical measurements, the acquired signal was stable in time, without peaks or fluctuations. The resulting calibration from this test is shown in Fig. 7.

The calibration curve of electrical measurements for strain has a

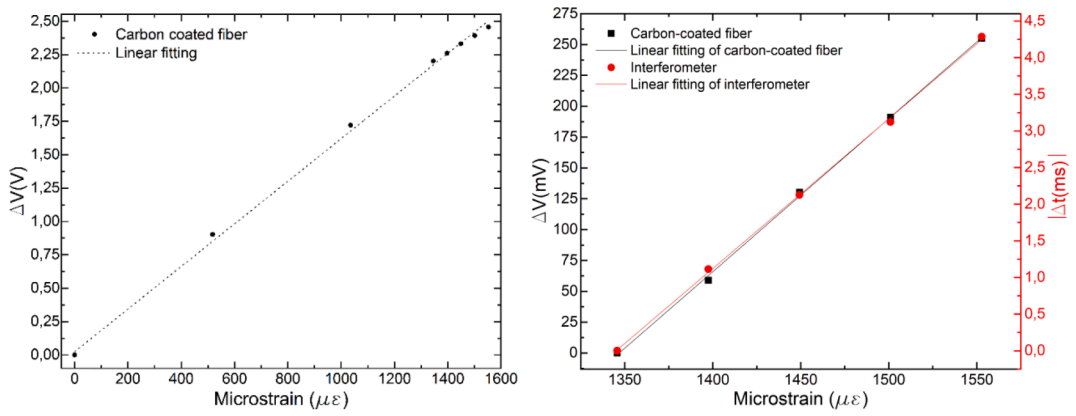

Fig. 7. Calibration curves of (a) electrical measurements from 0 to 1552.8 με and (b) optical and electrical measurements from 1345.75 to 1552.8 με.

linear behavior similar to that obtained from optical measurements. For electrical measurements, a Pearsońs r coefficient above 0.999 and a sensitivity of 1.582 mV/με with a maximum standard deviation of 7.94 mV were obtained. As a result, the correlation between the voltage variation (in mV) and strain (in με) is as follows:

$$\mu\varepsilon = 631.1\Delta V - 25.799 \tag{4}$$

Regarding optical measurements, the sensitivity of the interferometer was 0.0207 ms/με with a Pearsońs r coefficient above 0.999 as well. These results are in good agreement with those that can be obtained from the mathematical models of low coherence interferometers in [22,23] and [24]. This fact demonstrates that the carbon coating does not affect the transmission of light and validates the feasibility of the proposed operating principle.

3.2. Vibration measurements

The second test consisted in subjecting the carbon-coated fiber to low frequency vibrations. Such range is of interest in several applications as structural health monitoring, seismology [34] or the aeronautical industry, for instance, where these vibrations are monitored during the internal inspection of composites used in flap and wing fabrication [35–37]. As a first approach, a segment of carbon-coated fiber was surface bonded to a 30 cm x 3 cm flexible methacrylate plate of 1 mm thickness that had been bent at an angle of 90° under heat. The latter substituted the arm of the interferometer that had been used for strain measurements in the previous test. In idle state, the resistance of this sample of carbon-coated fiber was 393.1 kΩ, which was taken as reference. The lower resistance value compared to the sample used for strain measurements (430.95 kΩ) is due to its shorter length. Vibrations were applied to the upper part of the methacrylate plate by means of a shaker that was connected to a function generator (Hewlett Packard 33120A) and an amplifier (Brüel & Kjaer). For its interrogation, the signal from the photoreceiver was acquired with the same analog oscilloscope as before (Tektronix TDS 3034), whereas the signal from the Wheatstone bridge was measured with a digital oscilloscope (PicoScope 5000 Series) in order to record several cycles of vibration. The schematic of the experimental setup is shown in Fig. 8.

The test consisted of emitting a sinusoidal waveform of 1 Vpp and varying its frequency from 5 Hz down to 100 mHz (the lowest frequency provided by the function generator). The results are shown in Fig. 9. In Fig. 9a, the electrical signal as a function of time of the three most representative cases is shown. It can be noticed that the carbon-coated fiber has been able to detect clearly every emitted frequency down to 100 mHz. In Fig. 9b, the FFT of all the tested cases is shown, which is the result of applying a low pass FFT signal filtering to the signal in time in Fig. 9a. The narrowness in width of the most prominent FFT component and the low level of the harmonic components should be highlighted, as these characteristics are directly related to the purity of the acquired signal. In fact, results suggest that it could be possible to measure

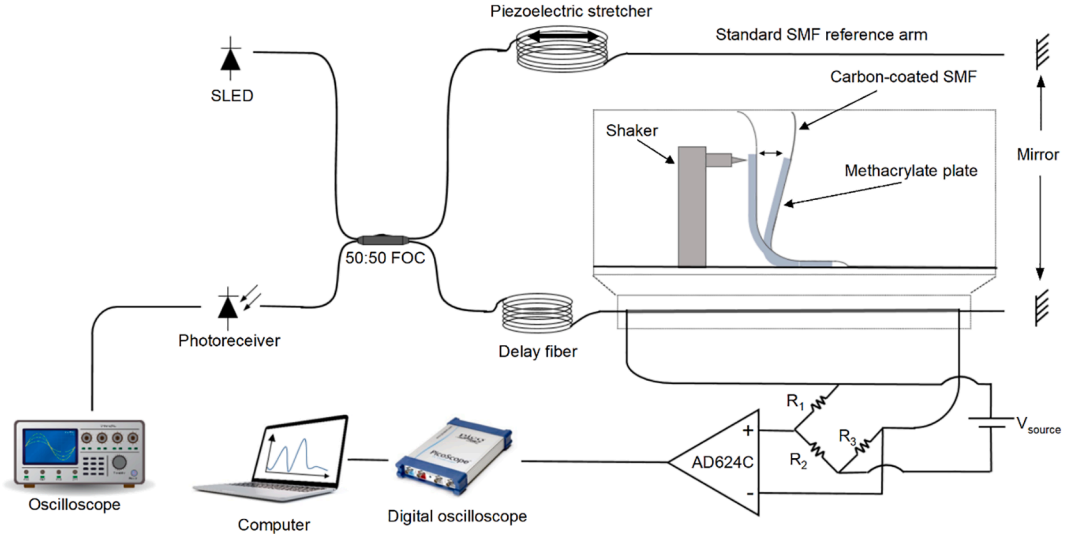

Fig. 8. Schematic of the experimental setup for vibration measurements.

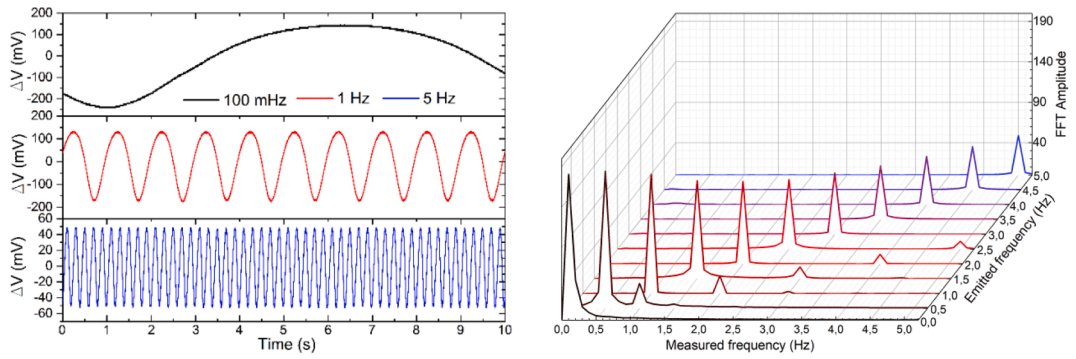

Fig. 9. Results of the vibration measurements. (a) Time response of the three most representative cases. (b) FFT amplitudes for the tested cases.

frequencies below 100 mHz with this method, as the signal to noise ratio (SNR) in the FFT amplitude of the most prominent component is significantly bigger than 3 times the second most prominent component in all cases. This criterion is commonly taken as a rule to define the Limit of Detection (LoD) [38].

4. Conclusions

In this work, we have reported on a carbon-coated fiber able to operate as an optical transmission medium and as an electrical sensor simultaneously. It consists of a standard SMF sleeved in a double coating aimed at providing protection and isolation from external elements. Such coating is comprised of an inner layer of carbon and an outer layer of polymer of 31.5 μm each. When the aforementioned fiber is subjected to mechanical stress, the physical properties of the carbon layer change according to it, modifying its resistance proportionally. The voltage variations caused by the former can be accurately measured and directly linked to the parameter causing the mechanical stress. This measurement process does not interfere with the light propagating through the SMF, which remains unaltered.

To demonstrate the feasibility of such operating principle, strain and vibration measurements were carried out in a low coherence interferometer in which the reference arm consisted of standard SMF and the arm exposed to the mechanical stress was comprised of this carbon-coated fiber. In this manner, electrical and optical signals could be measured simultaneously and compared to each other by means of a reliable and accurate technology such as interferometry. For strain, electrical measurements showed a linear behavior similar to that from optical measurements, reaching a sensitivity of 1.582 mV/με in the range from 0 με to 1552.8 με, whereas for vibrations, signals down to 100 mHz were recorded clearly.

Hence, results shown here indicate that electrical measurements are as accurate as optical ones with the advantage of not interfering or having impact on the optical signal, validating the feasibility of the operating principle based on using the carbon coating for sensing apart from providing protection. These features, added to its handling and interrogation ease and cost-effectiveness, make carbon-coated fibers appealing to be used in applications in which using the same fiber simultaneously for transmission and sensing is of interest. For instance, to be embedded in aeronautical composites, to be deployed in harsh environments as nuclear plants or submarine cables, or for structural health monitoring applications, as it allows optimizing resources, minimizing the level of intrusiveness and reducing the installation complexity. Alternatively, the dual optical and electronic measurements may be used to compensate the concurrent temperature/strain sensitive of the sensors.

CRediT authorship contribution statement

Josu Amorebieta: Writing – review & editing, Writing – original draft, Visualization, Validation, Methodology, Investigation, Formal analysis, Data curation. **Joao Pereira:** Validation, Software, Methodology, Investigation, Writing – review & editing. **Carolina Franciscangelis:** Methodology, Project administration, Supervision, Writing – review & editing. **Gaizka Durana:** Funding acquisition, Resources, Supervision, Writing – review & editing. **Joseba Zubia:** Writing – review & editing, Supervision, Project administration, Funding acquisition. **Joel Villatoro:** Writing – review & editing, Supervision, Project administration, Funding acquisition. **Walter Margulis:** Writing – review & editing, Writing – original draft, Visualization, Validation, Supervision, Resources, Project administration, Methodology, Investigation, Conceptualization.

Declaration of competing interest

The authors declare that they have no known competing financial interests or personal relationships that could have appeared to influence the work reported in this paper.

Data availability

Data will be made available on request.

Acknowledgements

This work was supported by the grants I + D + i/PID2021-122505OBC31, TED2021-129959B-C21, PDC2022-133053-C21, RTC2019-007194-4 and PDC2022-133885-100 funded by MCIN/AEI/10.13039/501100011033, by "ERDF A way of making Europe", by the "European Union Next Generation EU/PRTR". The research work is also supported by the Grant No. IT11452-22 and funded by the Basque Government, by ELKARTEK 2023 (μ4Smart-KK-2023/00016, MINAKU KK-2022/00080 and Ekohegaz II-KK-2023/00051) and by the University of the Basque Country. The work of Josu Amorebieta is funded by a PhD fellowship from the University of the Basque Country.

References

[1] P. Sharma, R.K. Arora, S. Pardeshi, M. Singh, "Fibre Optic Communications: An Overview." *International Journal of Emerging Technology and Advanced*, Engineering 3 (5) (2013) 474–479.
[2] P.J. Winzer, D.T. Neilson, A.R. Chraplyvy, Fiber-Optic transmission and networking: the previous 20 and the next 20 years [Invited], Opt. Express 26 (18) (2018) 24190–24239.
[3] N. Sabri, S.A. Aljunid, M.S. Salim, S. Fouad, Fiber Optic Sensors: Short Review and Applications, in: F.L. Gaol, K. Shrivastava, J. Akhtar (Eds.), Recent Trends in Physics of Material Science and Technology, Springer Singapore, Singapore, 2015, pp. 299–311.

[4] K.T.V. Grattan, T. Sun, Fiber optic sensor technology: an overview, Sens. Actuators, A 82 (1) (2000) 40–61.
[5] A. Wiberg, P. Perez-Millan, M.V. Andres, P.A. Andrekson, P.O. Hedekvist, Fiber-optic 40-Ghz Mm-Wave Link with 2.5-Gb/S data transmission, IEEE Photon. Technol. Lett. 17 (9) (2005) 1938–1940.
[6] B.G. Lee, D.M. Kuchta, F.E. Doany, C.L. Schow, P. Pepeljugoski, C. Baks, T. F. Taunay, B. Zhu, M.F. Yan, G.E. Oulundsen, D.S. Vaidya, W. Luo, N. Li, End-to-End multicore multimode fiber optic link operating up to 120 Gb/S, J. Lightwave Technol. 30 (6) (2012) 886–892.
[7] I. García, J. Zubia, G. Durana, G. Aldabaldetreku, M.A. Illarramendi, J. Villatoro, Optical fiber sensors for aircraft structural health monitoring, Sensors 15 (7) (2015) 15494–15519.
[8] C. Meunier, J.J. Guerin, M. Lequime, M. Rioual, E. Noel, D. Eguiazabal, D. Fleury, J. Maurin, R. Mongin, Industrial prototype of a fiber-optic sensor network for the thermal monitoring of the turbogenerator of a nuclear power plant-design, qualification, and settlement, J. Lightwave Technol. 13 (7) (1995) 1354–1361.
[9] S.Z. Yan, L.S. Chyan, Performance enhancement of botdr fiber optic sensor for oil and gas pipeline monitoring, Opt. Fiber Technol. 16 (2) (2010) 100–119.
[10] L. Bjerkan, Application of fiber-optic bragg grating sensors in monitoring environmental loads of overhead power transmission lines, Appl. Opt. 39 (4) (2000) 554–560.
[11] G. Tao, A.M. Stolyarov, A.F. Abouraddy, Multimaterial fibers, Int. J. Appl. Glas. Sci. 3 (4) (2012) 349–368.
[12] C. Li, W. Yang, M. Wang, Yu. Xiaoyang, J. Fan, Y. Xiong, Y. Yang, L. Li, A review of coating materials used to improve the performance of optical fiber sensors, Sensors 20 (15) (2020) 4215.
[13] P.J. Lemaire, E.A. Lindholm, A. Mendez, T.F. Morse, Hermetic optical fibers: carbon-coated fibers, Specialty Optical Fibers Handbook (2007) 453–490.
[14] S.Y. Chong, J.-R. Lee, C.-Y. Yun, H. Sohn, Design of copper/carbon-coated fiber bragg grating acoustic sensor net for integrated health monitoring of nuclear power plant, Nucl. Eng. Des. 241 (5) (2011) 1889–1898.
[15] A. Nedjalkov, J. Meyer, C. Waltermann, M. Reimer, A. Gillooly, M. Angelmahr, W. Schade, Direct inscription and evaluation of fiber bragg gratings in carbon-coated optical sensor glass fibers for harsh environment oil and gas applications, Appl. Opt. 57 (26) (2018) 7515–7525.
[16] K.E. Lu, G.S. Glaesemann, M.T. Lee, D.R. Powers, J.S. Abbott, Mechanical and hydrogen characteristics of hermetically coated optical fibre, Opt. Quant. Electron. 22 (3) (1990) 227–237.
[17] A. Sudirman, L. Norin, W. Margulis, Increased sensitivity in fiber-based spectroscopy using carbon-coated fiber, Opt. Express 20 (27) (2012) 28049–28055.
[18] R. Magalhães, A. Garcia-Ruiz, H.F. Martins, J. Pereira, W. Margulis, S. Martin-Lopez, M. Gonzalez-Herraez, Fiber-based distributed bolometry, Opt. Express 27 (4) (2019) 4317–4328.
[19] I. Kang, M.J. Schulz, J.H. Kim, V. Shanov, D. Shi, A carbon nanotube strain sensor for structural health monitoring, Smart Mater. Struct. 15 (3) (2006) 737–748.
[20] S.-T. Shiue, H.-H. Hsiao, T.-Y. Shen, H.-C. Lin, K.-M. Lin, Mechanical strength and thermally induced stress voids of carbon-coated optical fibers prepared by plasma enhanced chemical vapor deposition method with different hydrogen/methane ratio, Thin Solid Films 483 (1–2) (2005) 140–146.
[21] G.S. Glaesemann, Optical fiber mechanical reliability, White Paper 8002 (2017) 1–62.
[22] Y.-J. Rao, D.A. Jackson, Recent progress in fibre optic low-coherence interferometry, Meas. Sci. Technol. 7 (7) (1996) 981–999.
[23] Y.N. Ning, K.T.V. Grattan, A.W. Palmer, Fibre-optic interferometric systems using low-coherence light sources, Sens. Actuators, A 30 (3) (1992) 181–192.
[24] P.J. de Groot, A review of selected topics in interferometric optical metrology, Rep. Prog. Phys. 82 (5) (2019) 056101.
[25] T. Liu, C. Zhang, S. Wang, J. Jiang, K. Liu, X. Zhang, X. Wang, Simultaneous measurement of pressure and temperature based on adjustable line scanning polarized low-coherence interferometry with compensation plate, IEEE Photonics J. 10 (4) (2018) 1–9.
[26] A. Neef, V. Seyda, D. Herzog, C. Emmelmann, M. Schönleber, M. Kogel-Hollacher, Low coherence interferometry in selective laser melting, Phys. Procedia 56 (2014) 82–89.
[27] D. Inaudi, A. Elamari, L. Pflug, N. Gisin, J. Breguet, S. Vurpillot, Low-coherence deformation sensors for the monitoring of civil-engineering structures, Sens. Actuators, A 44 (2) (1994) 125–130.
[28] J. Park, J.-A. Kim, H. Ahn, J. Bae, J. Jin, A Review of Thickness Measurements of Thick Transparent Layers Using Optical Interferometry, Int. J. Precision Eng. Manuf. 20 (3) (2019) 463–477.
[29] W.J. Brown, J.W. Pyhtila, N.G. Terry, K.J. Chalut, T.A. D' Amico, T.A. Sporn, J. V. Obando, A. Wax, Review and Recent Development of Angle-Resolved Low-Coherence Interferometry for Detection of Precancerous Cells in Human Esophageal Epithelium, IEEE J. Sel. Top. Quantum Electron. 14 (1) (2008) 88–97.
[30] N.V. Iftimia, B.E. Bouma, M.B. Pitman, B. Goldberg, J. Bressner, G.J. Tearney, A portable, low coherence interferometry based instrument for fine needle aspiration biopsy guidance, Rev. Sci. Instrum. 76 (6) (2005) 064301.
[31] A.M. Zysk, S.G. Adie, J.J. Armstrong, M.S. Leigh, A. Paduch, D.D. Sampson, F. T. Nguyen, S.A. Boppart, Needle-based refractive index measurement using low-coherence interferometry, Opt. Lett. 32 (4) (2007) 385–387.
[32] P. Jansz, S. Richardson, G. Wild, S. Hinckley, Modeling of low coherence interferometry using broadband multi-gaussian light sources, Photonic Sensors 2 (2012) 247–258.
[33] X. Chapeleau, D. Leduc, C. Lupi, V. Gaillard, C. Boisrobert, Low coherence interferometry, Measurements Using Optic and RF Waves (2013) 81–112.
[34] J. Amorebieta, A. Ortega-Gomez, G. Durana, R. Fernández, E. Antonio-Lopez, A. Schülzgen, J. Zubia, R. Amezcua-Correa, J. Villatoro, Highly sensitive multicore fiber accelerometer for low frequency vibration sensing, Sci. Rep. 10 (1) (2020) 16180.
[35] A. Cusano, P. Capoluongo, S. Campopiano, A. Cutolo, M. Giordano, F. Felli, A. Paolozzi, M. Caponero, Experimental modal analysis of an aircraft model wing by embedded fiber bragg grating sensors, IEEE Sens. J. 6 (1) (2006) 67–77.
[36] D. Goutaudier, D. Gendre, V. Kehr-Candille, R. Ohayon, Long-range impact localization with a frequency domain triangulation technique: application to a large aircraft composite panel, Compos. Struct. 238 (2020) 111973.
[37] P.A. Ochôa, R.M. Groves, R. Benedictus, Effects of high-amplitude low-frequency structural vibrations and machinery sound waves on ultrasonic guided wave propagation for health monitoring of composite aircraft primary structures, J. Sound Vib. 475 (2020) 115289.
[38] A. Shrivastava, V.B. Gupta, Methods for the determination of limit of detection and limit of quantitation of the analytical methods, Chronicles of Young Scientists 2 (1) (2011) 21–25.